Electronic Supplementary Material (ESI)

Rhodium single-atom catalysts with enhanced electrocatalytic hydrogen evolution performance

Zhipeng Yu,†[a,b] Junyuan Xu,†[a] Siquan Feng,†[c,d] Xiangen Song,[c] Oleksandr Bondarchuk,[a] Joaquim L. Faria,[b] Yunjie Ding*[c,e] and Lifeng Liu*[a]

[a.] International Iberian Nanotechnology Laboratory (INL), Avenida Mestre Jose Veiga, 4715-330 Braga, Portugal

[b.] Laboratory of Separation and Reaction Engineering – Laboratory of Catalysis and Materials (LSRE-LCM), Faculdade de Engenharia, Universidade do Porto, Rua Dr. Roberto Frias, 4200-465 Porto, Portugal

[c.] Dalian National Laboratory for Clean Energy, Dalian Institute of Chemical Physics, Chinese Academy of Sciences, 116023 Dalian, China

[d.] University of Chinese Academy of Sciences, 100049 Beijing, China

[e.] State Key Laboratory of Catalysis, Dalian Institute of Chemical Physics, Chinese Academy of Sciences, 116023 Dalian, China

† These authors contributed equally to this work.

* Corresponding author email. dyj@dicp.ac.cn (Y. J. Ding) lifeng.liu@inl.int (L. Liu)

Experimental procedures

Preparation of the Rh_1/AC catalysts:

The Rh_1/AC catalysts were prepared according to the "top-down" approach reported previously.[S1] Firstly, the coconut activated carbon (AC) was ground to 40-60 mesh and washed with deionized (DI) water at 80 °C. The electrical conductivity of the DI water is below 20 μS cm^{-1}. The AC powders were then dried in static air at 120 °C for 12 h to obtain AC support ready for use to prepare Rh_1/AC. Secondly, 1.35 g $RhCl_3 \cdot nH_2O$ with 37 wt% metal content was dissolved in 15 mL deionized water to obtain precursor solutions. Subsequently, 10 g dried AC powders were added in, and the mixture was stirred continuously until no bubbles could be discerned by naked eyes. Afterwards, the mixture of the solution and AC was statically dried at 90 °C until all the solvent was volatilized, followed by further drying at 120 °C overnight to completely remove the residual water. Thirdly, the collected powders were loaded in a quartz tubular reactor, calcined at 300 °C for 2 h in a flow of N_2 (100 mL/min), and then continuously reduced in high-purity H_2 at the same temperature for 2 h, which resulted in the formation of Rh NPs supported on AC (Rh/AC). Lastly, the as-obtained Rh/AC was treated in a mixture of CO/CH_3I at 240 °C for 6 h (CO passed through a bottle filled with CH_3I at 25 °C with a flow rate of 30 mL/min), during which the re-dispersion of Rh happened that led to the formation of Rh SACs (Rh_1/AC). The reactor was cooled down to room temperature in a flow of CO after the chemical reaction.

Materials Characterization:

The morphology of AC, Rh/AC, Rh_1/AC catalysts was characterized by scanning electron microscopy (SEM, FEI Quanta 650 FEG microscope equipped with INCA 350 spectrometer) and transmission electron microscopy (TEM, FEI ChemiSTEM 80-200,

probe corrected). The X-ray diffraction (XRD) experiment was conducted on an X'Pert PRO diffractometer (PANalytical) set at 45 kV and 40 mA, using Cu K_α radiation (λ = 1.541874 Å) and a PIXcel detector. Data were collected with the Bragg–Brentano configuration in the 2θ range of 30 – 80° at a scan speed of 0.011° s^{-1}. X-ray photoelectron spectroscopy (XPS) characterization was carried out on an ESCALAB 250Xi instrument with monochromated Al K_α (1486.6 eV) X-ray source.

Electrocatalytic tests:

The catalyst ink was prepared by ultrasonically dispersing 5 mg of Rh_1/AC catalysts with Rh loading of 5 wt% into 500 µL of ethanol + 50 µL of Nafion® (Sigma, 5 wt%) solution. To prepare an electrode for electrocatalytic tests, 6.6 µL of catalyst ink was loaded on a polished glassy carbon (GC) electrode with an exposed area of 0.2 cm^2. The Rh loading can be calculated as follows:

$$C = \frac{5\ mg\ \times 6.6\ \mu L\ \times 5\%}{(500\ \mu L + 50\ \mu L) \times 0.2\ cm^2} = 15\ \mu g\ cm^{-2} \quad \text{(S1)}$$

For comparison, the HER performances of commercial Pt/C (20 wt%, Johnson Matthey) catalysts, Rh/AC and AC support control samples were also investigated. The working electrode was prepared according to the procedures similar to what described above. The metal loadings of Pt/C and Rh/AC were 60 and 15 µg cm^{-2}, respectively. The electrodes loaded with catalysts were dried at room temperature (ca. 25 °C) naturally in the air.

All the electrocatalytic tests were carried out in a three-electrode configuration at room temperature using a Biologic VMP-3 potentiostat/galvanostat. A graphite rod and a saturated calomel electrode (SCE) were utilized as counter and reference electrodes, respectively. The SCE reference was calibrated before each measurement in pure H_2-

saturated 0.5 M H_2SO_4 solution using a clean Pt wire as the working electrode. Unless otherwise stated, all potentials are reported versus RHE by converting the measured potentials to the RHE scale according to the following equation:

$$E_{RHE} = E_{SCE} + 0.059 \times pH + 0.244 \quad \text{(S2)}$$

Linear scan voltammetry (LSV) was performed at a scan rate of 5 mV s^{-1} in 1.0 M NaOH. *iR*-correction (85%) was made to compensate for the voltage drop between the reference and working electrodes, which was measured by single-point high-frequency impedance measurement. The cyclic durability of Rh_1/AC, Rh/AC and commercial Pt/C catalysts were studied and compared by repetitive cyclic voltammetry (CV) scans. The potential was scanned between −0.36 and 0.14 V *vs* RHE at a scan rate of 100 mV s^{-1}. After 45000 cycles, a CV curve was recorded at 5 mV s^{-1}. Furthermore, the stability of Rh_1/AC, Rh/AC and commercial Pt/C catalysts was assessed using chronopotentiometry (CP) at a constant current density of −10 mA cm^{-2}. All LSV, CV and CP curves were recorded in the electrolyte constantly bubbled with Ar/H_2 (5% H_2, v/v).

The electrochemically active surface area (ECSA) of the catalysts was estimated from the electrochemical double-layer capacitance (C_{dl}) of the catalysts' surface. The C_{dl} value was derived by performing CV in the potential range of 0.34 – 0.54 V *vs.* RHE (non-Faradaic potential range) at different scan rates (ν) of 10, 20, 30, 40, 50, 60, 70, 80, 90 and 100 mV s^{-1}, followed by extracting the slope from the resulting $|j_a-j_c|/2$ *vs* ν plots, where j_a and j_c represent the anodic and cathodic current at 0.44 V *vs.* RHE. The ECSA can be then calculated by dividing the obtained C_{dl} by the specific capacitance (C_s) of catalytic materials, which is usually 0.04 mF cm^{-2} in strongly alkaline solution (e.g. 1 M NaOH used in this work) for most flat metal electrodes as explained by Jaramillo et al. in

their previous work (pages 8-9, Supporting Information, J. Am. Chem. Soc. 2013, 135, 16977)[S2]

$$ECSA = C_{dl} / 0.04\ mF\ cm^{-2} \quad (S3)$$

The electrochemical impedance spectroscopy (EIS) measurements were carried out at an overpotential of 50 mV in the frequency range of 10^5 – 0.01 Hz with a 10 mV sinusoidal perturbation.

The turnover frequency (TOF) of the catalysts was calculated according to the following formula:

$$TOF\ (s^{-1}) = \frac{j \times A}{2 \times F \times n} \quad (S4)$$

where j (A cm^{-2}) is the current density at a given overpotential, A = 0.2 cm^2 is the geometric surface area of the electrode, F = 96500 C mol^{-1} stands for the Faraday constant, n (mol) is mole number of Rh or Pt loaded on the GC electrode. All metal cations in the catalyst were assumed to be catalytically active, so the calculated values represent the lower limits of TOF.

The volume of hydrogen gas evolved from the electrode was collected by the water displacement method in a home-made H-type cell. The Faradaic efficiency of the HER was then calculated using the charge for hydrogen evolution divided by the total charge passed in a given period of time, assuming two electrons are involved in producing one hydrogen molecule.

Supplementary figures

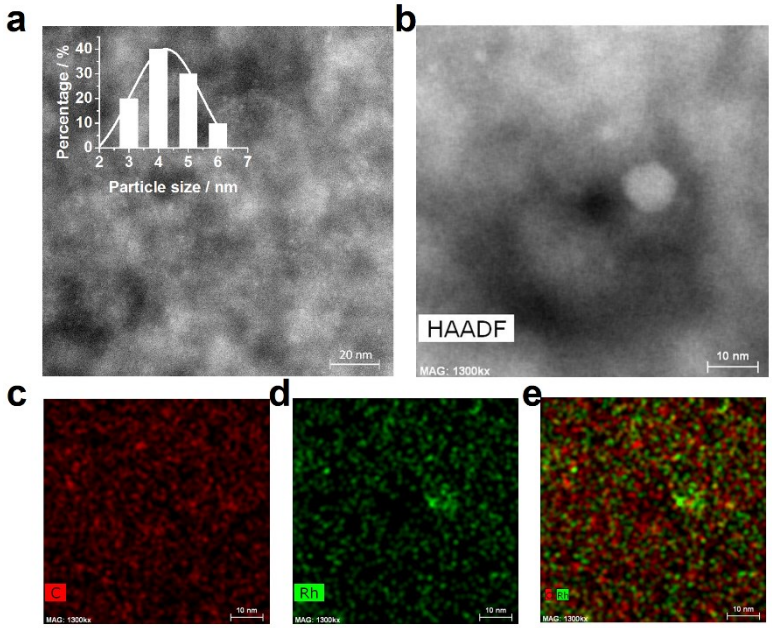

Fig. S1 (a, b) HAADF-STEM images of the as-prepared Rh/AC catalysts. (c-e) EDX elemental maps of (c) C, (d) Rh, and (e) their overlay.

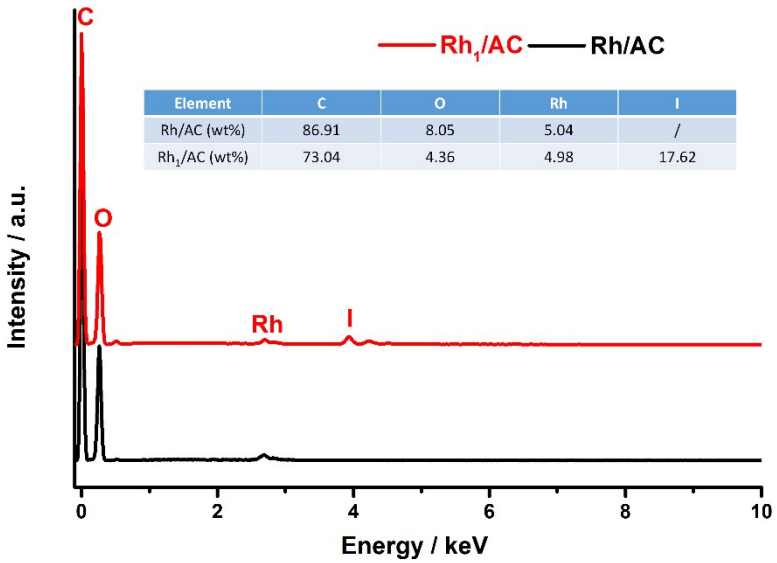

Element	C	O	Rh	I
Rh/AC (wt%)	86.91	8.05	5.04	/
Rh_1/AC (wt%)	73.04	4.36	4.98	17.62

Fig. S2 SEM-EDX spectra of the as-prepared Rh/AC and Rh_1/AC catalysts. The quantitative analysis confirmed the mass loading of Rh on AC (ca. 5 wt%).

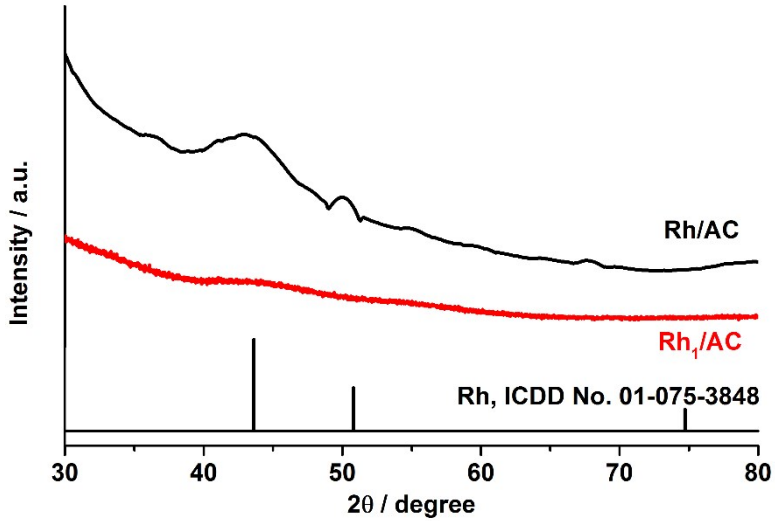

Fig. S3 XRD patterns of the as-prepared Rh/AC and Rh_1/AC catalysts.

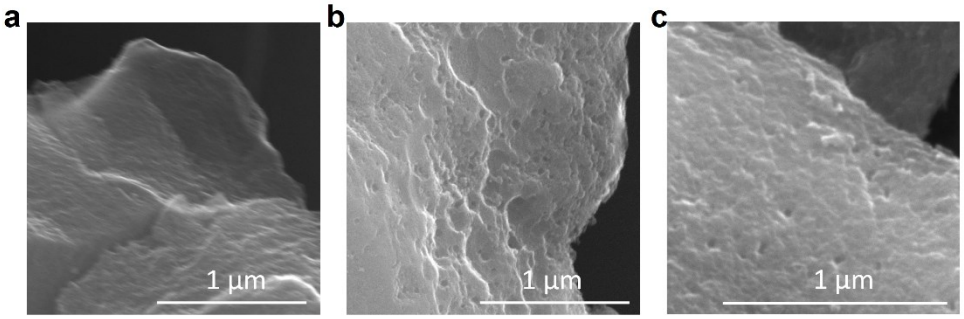

Fig. S4 SEM images of the as-prepared (a) AC, (b) Rh/AC and (c) Rh_1/AC.

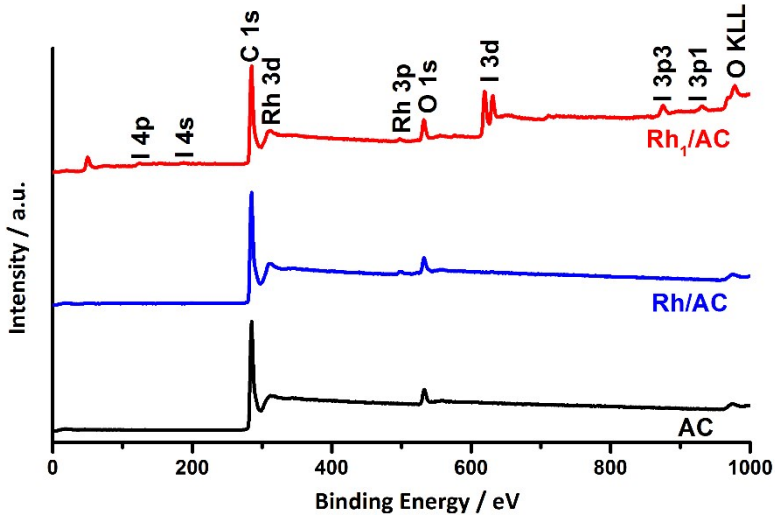

Fig. S5 XPS survey spectra of the AC, Rh/AC and Rh_1/AC.

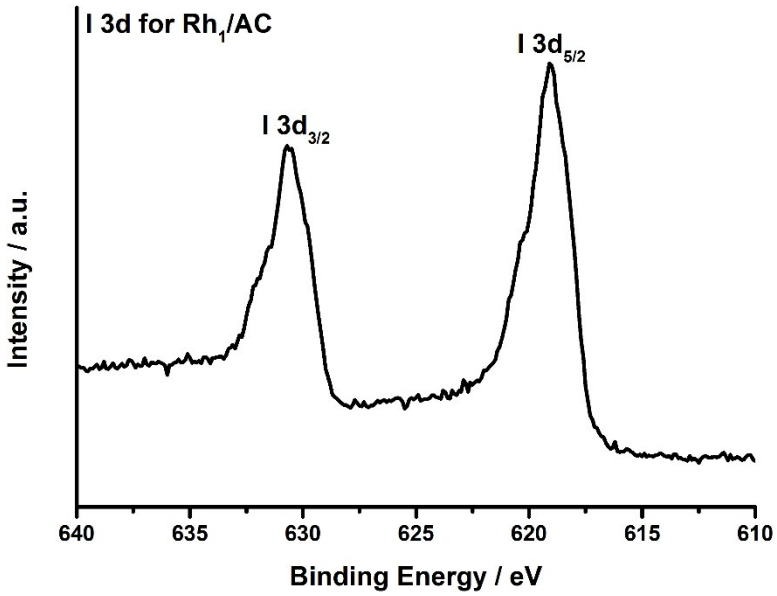

Fig. S6 XPS spectrum of I3d for Rh_1/AC.

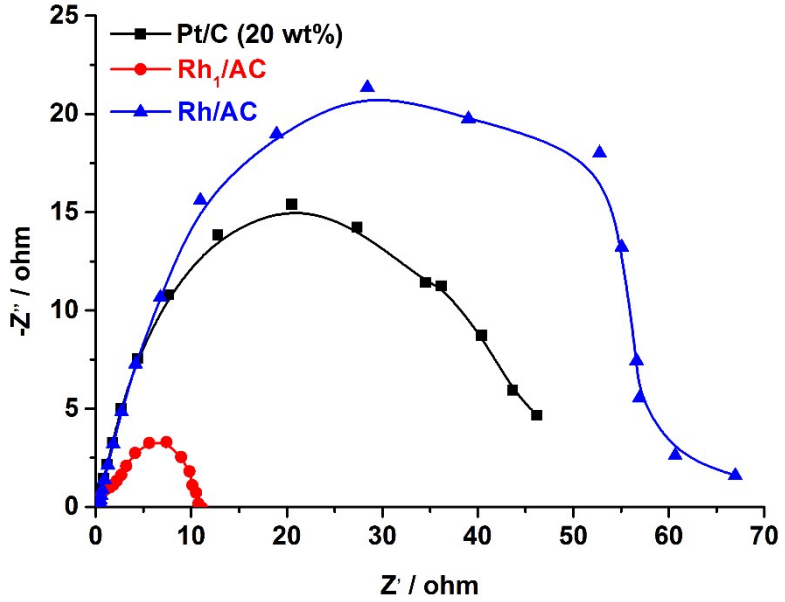

Fig. S7 Nyquist plots of all catalysts measured at an overpotential of 50 mV.

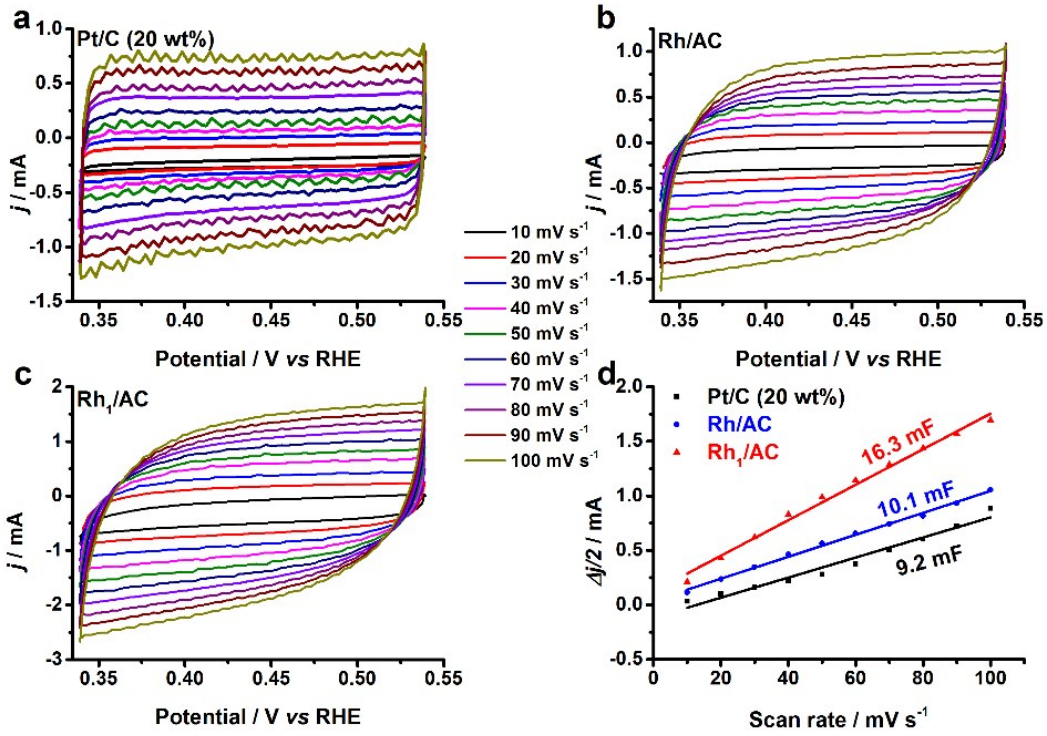

Fig. S8 Electrochemical CV curves of (a) Pt/C, (b) Rh/AC and (c) Rh_1/AC, recorded at different scan rates of 10, 20, 30, 40, 50, 60, 70, 80, 90 and 100 mV s^{-1}. (d) Plots of the capacitive currents as a function of the scan rate for all the catalysts.

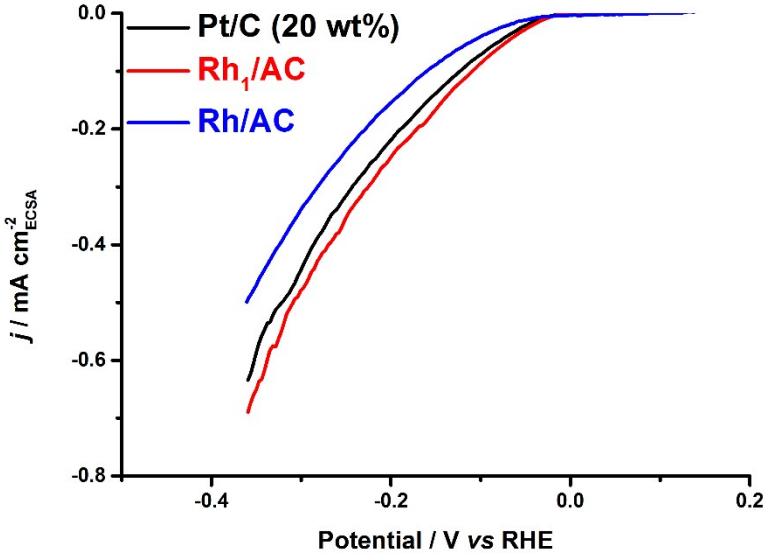

Fig. S9 Specific activity Rh_1/AC and other control catalysts.

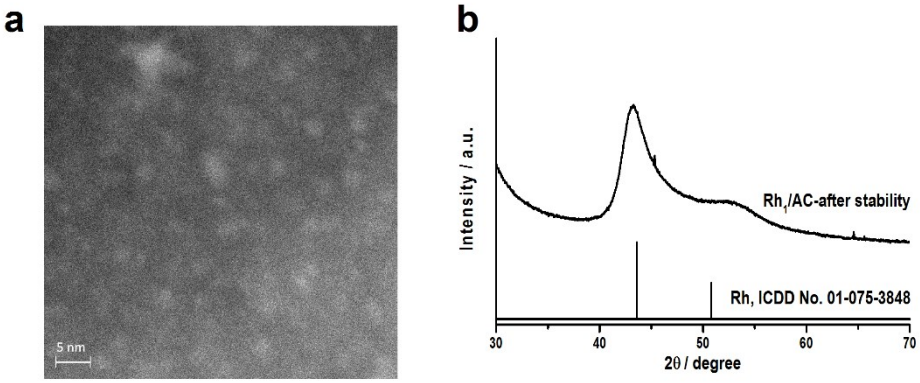

Fig. S10 (a) STEM image and (b) XRD pattern of Rh_1/AC after the extended stability test at −10 mA cm^{-2} for 290 h.

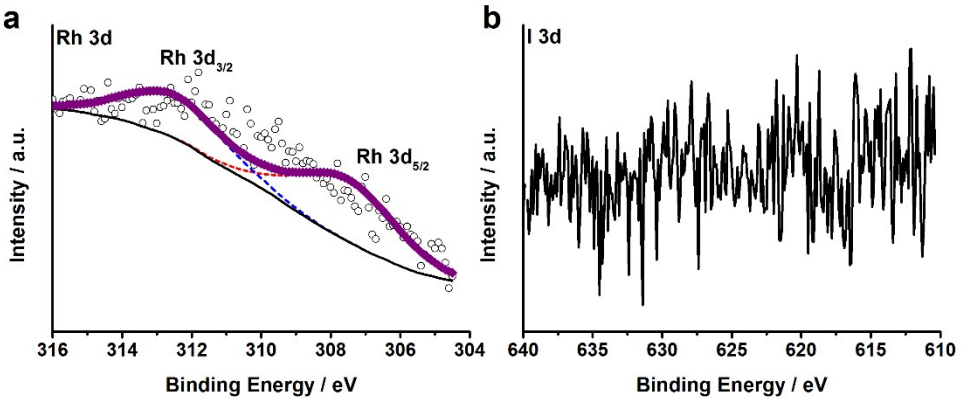

Fig. S11 XPS spectra of (a) Rh3d and (b) I3d for Rh_1/AC after the extended stability test at –10 mA cm^{-2} for 290 h.

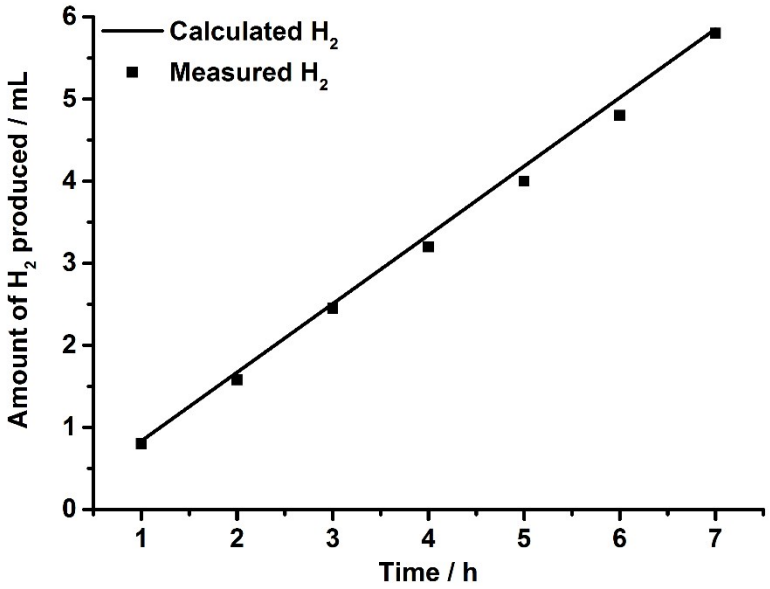

Fig. S12 Experimentally measured and calculated volumes of H_2 gas evolved from Rh_1/AC at a fixed current density of -10 mA cm^{-2}.

Table S1. Comparison of the HER activity of Rh_1/AC with other SACs tested in alkaline solutions recently reported in the literature.

Catalysts	Overpotential @ j = −10 mA cm^{-2} (η_{10}, mV)	Tafel slope / mV dec^{-1}	Ref.
Rh_1/AC	48	33	This work
Pt@PCM	139	73.6	S3
SANi-PtNWs	70	60.3	S4
Ru@Co SAs/N–C	7	30	S5
Ru-MoS_2/CC	41	114	S6
Rh@NG	33	30	S7
Co_1/PCN	89	52	S8
$Mo_1N_1C_2$	132	90	S9
Co_1N_x/C	170	75	S10
Pt/np-$Co_{0.85}Se$	58	39	S11
Ru-NC-700	47	14	S12
Pt_1/N-C	46	36.8	S13
Ni_{SA}-MoS_2/CC	95	75	S14
SA-Ru-MoS_2	76	21	S15
Ru_{SA}-N-S-$Ti_3C_2T_x$	99	/	S16
W-SAC	85	53	S17

References

S1. S. Q. Feng, X. G. Song, Y. Liu, X. S. Lin, L. Yan, S. Y. Liu, W. R. Dong, X. M. Yang, Z. Jiang and Y. J. Ding, *Nat. Commun.*, 2019, **10**, 5281.

S2. C. C. L. McCrory, S. H. Jung, J. C. Peters and T. F. Jaramillo, *J. Am. Chem. Soc.,* 2013, **135**, 16977-16987.

S3. H. Zhang, P. An, W. Zhou, B. Y. Guan, P. Zhang, J. Dong and X. W. Lou, *Sci. Adv.*, 2018, **4**, eaao6657.

S4. M. Li, K. Duanmu, C. Wan, T. Cheng, L. Zhang, S. Dai, W. Chen, Z. Zhao, P. Li, H. Fei, Y. Zhu, R. Yu, J. Luo, K. Zang, Z. Lin, M. Ding, J. Huang, H. Sun, J. Guo, X. Pan, W. A. Goddard, P. Sautet, Y. Huang and X. Duan, *Nat. Catal.*, 2019, **2**, 495-503.

S5. S. Yuan, Z. Pu, H. Zhou, J. Yu, I. S. Amiinu, J. Zhu, Q. Liang, J. Yang, D. He, Z. Hu, G. Van Tendeloo and S. Mu, *Nano Energy*, 2019, **59**, 472-480.

S6. D. Wang, Q. Li, C. Han, Z. Xing and X. Yang, *Appl. Catal. B Environ.*, 2019, **249**, 91-97.

S7. J. Guan, X. Wen, Q. Zhang and Z. Duan, *Carbon*, 2020, **164**, 121-128.

S8. L. Cao, Q. Luo, W. Liu, Y. Lin, X. Liu, Y. Cao, W. Zhang, Y. Wu, J. Yang, T. Yao and S. Wei, *Nat. Catal.*, 2019, **2**, 134-141.

S9. W. Chen, J. Pei, C. T. He, J. Wan, H. Ren, Y. Zhu, Y. Wang, J. Dong, S. Tian, W. C. Cheong, S. Lu, L. Zheng, X. Zheng, W. Yan, Z. Zhuang, C. Chen, Q. Peng, D. Wang and Y. Li, *Angew. Chem. Int. Ed.*, 2017, **56**, 16086-16090.

S10. H. W. Liang, S. Brüller, R. Dong, J. Zhang, X. Feng and K. Müllen, *Nat. Commun.*, 2015, **6**, 7992.

S11. K. Jiang, B. Liu, M. Luo, S. Ning, M. Peng, Y. Zhao, Y. R. Lu, T. S. Chan, F. M. F. de Groot and Y. Tan, *Nat. Commun.*, 2019, **10**, 1743.

S12. B. Lu, L. Guo, F. Wu, Y. Peng, J. E. Lu, T. J. Smart, N. Wang, Y. Z. Finfrock, D. Morris, P. Zhang, N. Li, P. Gao, Y. Ping and S. Chen, *Nat. Commun.*, 2019, **10**, 631.

S13. S. Fang, X. Zhu, X. Liu, J. Gu, W. Liu, D. Wang, W. Zhang, Y. Lin, J. Lu, S. Wei, Y. Li and T. Yao, *Nat. Commun.*, 2020, **11**, 1029.

S14. Q. Wang, Z. L. Zhao, S. Dong, D. He, M. J. Lawrence, S. Han, C. Cai, S. Xiang, P. Rodriguez, B. Xiang, Z. Wang, Y. Liang and M. Gu, *Nano Energy*, 2018, **53**, 458-467.

S15. J. Zhang, X. Xu, L. Yang, D. Cheng and D. Cao, *Small Methods*, 2019, **3**, 1900653.

S16. V. Ramalingam, P. Varadhan, H. C. Fu, H. Kim, D. Zhang, S. Chen, L. Song, D. Ma, Y. Wang, H. N. Alshareef and J. H. He, *Adv. Mater.*, 2019, **31**, 1903841.

S17. W. Chen, J. Pei, C. T. He, J. Wan, H. Ren, Y. Wang, J. Dong, K. Wu, W. C. Cheong, J. Mao, X. Zheng, W. Yan, Z. Zhuang, C. Chen, Q. Peng, D. Wang and Y. Li, *Adv. Mater.*, 2018, **30**, 1800396.